

# Single Two-Electron Transfers vs Successive One-Electron Transfers in Polyconjugated Systems Illustrated by the Electrochemical Oxidation and Reduction of Carotenoids

Philippe Hapiot,<sup>1a,b</sup> Lowell D. Kispert,<sup>\*,1c</sup> Valery V. Konovalov,<sup>1a,d</sup> and Jean-Michel Savéant<sup>\*,1a</sup>

Contribution from the Department of Chemistry, Box 870336, University of Alabama, Tuscaloosa, Alabama 35487, and the Laboratoire d'Electrochimie Moléculaire, Unité mixte de Recherche Université-CNRS No. 7591, Université de Paris 7 -Denis Diderot, Case Courier 7107, 2 Place Jussieu, 75251 Paris Cedex 05, France

Received March 6, 2001

**Abstract:** Examination of cyclic voltammetric responses reveals that inversion of the standard potentials of the first and second electron transfers occurs in the oxidation of  $\beta$ -carotene and 15,15'-didehydro- $\beta$ -carotene (but not in their reduction) as well as in the reduction of canthaxanthin (but not in its oxidation). The factors that control potential inversion in these systems, and more generally in symmetrical molecules containing conjugated long chains, are investigated by quantum chemical calculations. Two main interconnected effects emerge. One is the localization of the charges in the di-ion toward the ends of the molecule at a large distance from one another, thus minimizing Coulombic repulsion. The same effect favors the solvation of the di-ion providing additional stabilization. In contrast, the charge in the ion radical is delocalized over the whole molecular framework, thus disfavoring its stabilization by interaction with the solvent. The combination of the two solvation effects allows potential inversion to occur as opposed to the case where the two electrophores are linked by a saturated bridge where potential inversion cannot occur. Localization of the charges in the di-ion, and thus potential inversion, is favored by the presence of electron-accepting terminal groups for reductions (as the two carbonyl groups in canthaxanthin) and of hole-accepting terminal groups for oxidations (as in  $\beta$ -carotene).

## Introduction

Interest in the electrochemistry of carotenoids resides in the determination of their redox properties, which help to understand their role in biosystems, particularly in photosynthesis.<sup>2</sup> In this connection, it has been suggested that carotenoids can act as conductors to shuttle electrons through biological membranes.<sup>3</sup> This is also the case in triads mimicking photosynthetic systems.<sup>4</sup> Related to the conducting properties<sup>5</sup> is the question of the ease, in the thermodynamic sense, of the addition or removal of a second electron to such polyenic systems relative to the addition or removal of a first electron.

The first reports<sup>6</sup> on the electrochemical oxidation of  $\beta$ -carotene (**1**, Chart 1) indicated the exchange of two electrons per molecule, which was confirmed using simultaneous EPR and cyclic voltammetry technique<sup>7</sup> and also observed for longer chain carotene derivatives.<sup>8</sup> On the reduction side, the case of the dicarbonyl derivative, canthaxanthin (**3**, Chart 1) is not clear since coulometry indicates a two-electron stoichiometry at high concentration and a one-electron stoichiometry at low concentration.<sup>9</sup>

With most molecules, the second electron is more difficult to add (or to remove) than the first, resulting, in cyclic voltammetry, in two successive one-electron reversible waves. The reason for this behavior is the large Coulombic repulsion between the two injected charges, which is only partially compensated by the increase of the solvation free energy upon going from the starting molecule to the radical mono-ion and

(1) (a) Université de Paris 7—Denis Diderot. (b) Present address: Laboratoire d'Electrochimie, Synthèse et Electrosynthèse Organique UMR 6510 Université de Rennes 1, Campus de Beaulieu, 35042 Rennes Cedex France. (c) University of Alabama. (d) On leave from the Institute of Chemical Kinetics and Combustion SB RAS, 630090 Novosibirsk, Russia. Present address: Department of Physics, University of Alabama at Birmingham, CH310, Birmingham, AL 35294.

(2) (a) Frank, H. A.; Violette, C. A.; Trautman, J. K.; Shreve, A. P.; Owens, T. G.; Albrecht, A. C. *Pure Appl. Chem.* **1991**, *63*, 109. (b) Koyama, Y. *J. Photochem. Photobiol. B* **1991**, *9*, 265. (c) Bialek-Bylka, G. E.; Tomo, T.; Satoh, K.; Koyama, Y. *FEBS Lett.* **1995**, *363*, 137. (d) Bensasson, R. V.; Land, E. J.; Truscott, T. G. *Excited States and Free Radicals in Biology and Medicine*; Oxford University Press: Oxford, U.K., 1993.

(3) (a) Platt, J. R. *Science* **1959**, *129*, 372. (b) Kuhn, H. *Chem. Phys. Lipids* **1972**, *8*, 401. (c) Berns, D. S. *Photochem. Photobiol.* **1976**, *24*, 117. (d) Kugimiya, S.-I.; Iasrak, T.; Blanchard-Desce, M.; Lehn, J. M. *J. Chem. Soc. Chem. Commun.* **1991**, 1179.

(4) (a) Seta, P.; Bienvenue, E.; Moore, A. L.; Mathis, P.; Bensasson, R. V.; Liddel, P.; Pessiki, P. J.; Joy, A.; Moore T. A.; Gust, D. *Nature* **1984**, *307*, 630. (b) Seta, P.; Bienvenue, E.; Moore, A. L.; Moore T. A.; Gust, D. *Electrochem. Acta* **1989**, *34*, 1723.

(5) Tolbert, L. M. *Acc. Chem. Res.* **1992**, *25*, 561.

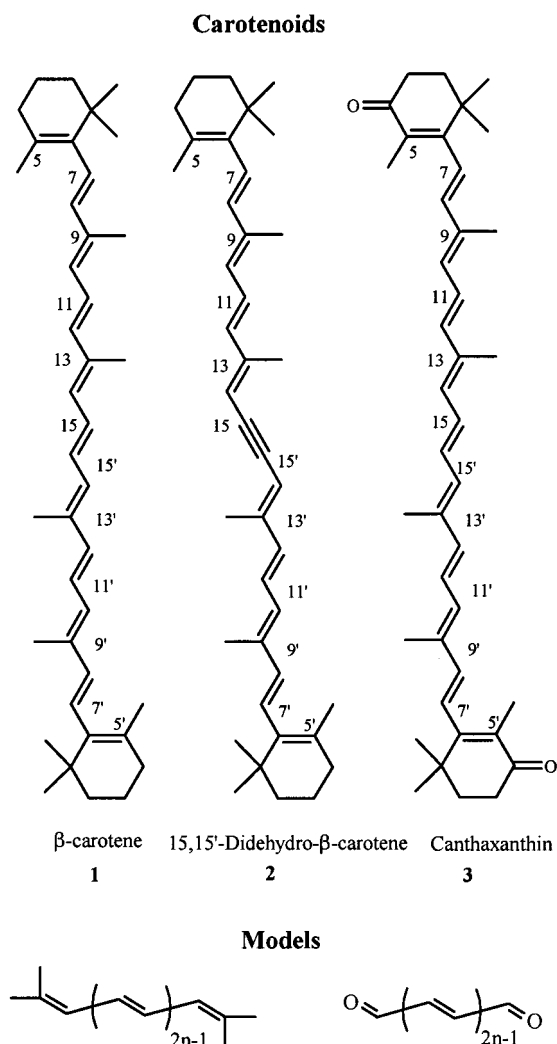
(6) (a) Mairanovsky, V. G.; Engovatov, A. A.; Ioffe, N. T.; Samokhvalov, G. I. *J. Electroanal. Chem.* **1975**, *66*, 123. (b) Park, S.-M. *J. Electrochem. Soc.* **1978**, 216.

(7) (a) Jeevarajan, A. S.; Khaled, M.; Kispert, L. D. *Chem. Phys. Lett.* **1994**, *228*, 340. (b) Jeevarajan, J. A.; Kispert, L. D. *J. Electroanal. Chem.* **1996**, *411*, 57. (c) Jeevarajan, J. A.; Jeevarajan, A. S.; Kispert, L. D. *J. Chem. Soc., Faraday Trans.* **1996**, *92*, 1757. (d) Gao, G.; Wei, C. C.; Jeevarajan, A. S.; Kispert, L. D. *J. Phys. Chem.* **1996**, *100*, 5362. (e) Liu, D.; Gao, G.; Kispert, L. D. *J. Electroanal. Chem.* **2000**, *488*, 140.

(8) Broszeit, G.; Diepenbrock, F.; Gräf, O.; Hecht, D.; Heinze, J.; Martin, H.-D.; Mayer, B.; Schaper, K.; Smie, A.; Strehlow, H. H. *Liebigs Ann.* **1997**, 2205.

(9) (a) Hall, E. A. H.; Moss, G. P.; Utley, J. H. P.; Weedon, B. C. L. *Chem. Commun.* **1976**, 586. (b) Utley, J. H. P. In *Carotenoid Chemistry and Biochemistry*; Britton, G., Goodwin, T. W., Eds.; Pergamon Press: Oxford, U.K., 1982; pp 97–105.

Chart 1



then to the di-ion. In contrast, molecules bearing two identical electrophores bound together by a long saturated chain, give rise to a single two-electron wave, which is exactly double the one-electron reversible wave characterizing each electrophore.<sup>10</sup> This behavior results from the fact that, as the distance between the two groups increases, the two electrophores becomes electronically independent and the Coulombic repulsion between the two charges in the di-ion becomes smaller and smaller.<sup>10</sup> There are, in addition, several systems for which it has been shown that the removal of the second electron is significantly easier than the first, as measured by electrochemical methods<sup>11</sup> or by spectral determination of the disproportionation rate constant,  $K_d$ .<sup>12</sup>

$$\frac{RT}{F} \ln K_d = \pm(E_1^0 - E_2^0) \quad \begin{array}{l} (+) \text{ for oxidation} \\ (-) \text{ for reduction} \end{array} \quad (1)$$

(10) (a) Then, the two standard potentials are not exactly the same but differ by  $(RT/F) \ln 4$  (35.6 mV at 25 °C) because there are two possibilities for adding (or removing) the second electron resulting in an entropy change of  $R \ln 4$  for the disproportionation reaction.<sup>10b</sup> This analysis has further been extended to the case of molecules bearing  $n$  identical electrophores.<sup>10c</sup> (b) Ammar, F.; Savéant, J.-M. *J. Electroanal. Chem.* **1973**, *43*, 115. (c) Flanagan, J. B.; Margel, S.; Bard, A. J.; Anson, F. C. *J. Am. Chem. Soc.* **1978**, *100*, 4248.

(11) (a) Myers, R. L.; Shain, I. *Anal. Chem.* **1969**, *41*, 980. (b) Andrieux, C.P.; Savéant, J.-M. *J. Electroanal. Chem.* **1974**, *57*, 27. (c) Grzeszczuk, M.; Smith, D. E. *J. Electroanal. Chem.* **1984**, *162*, 189.

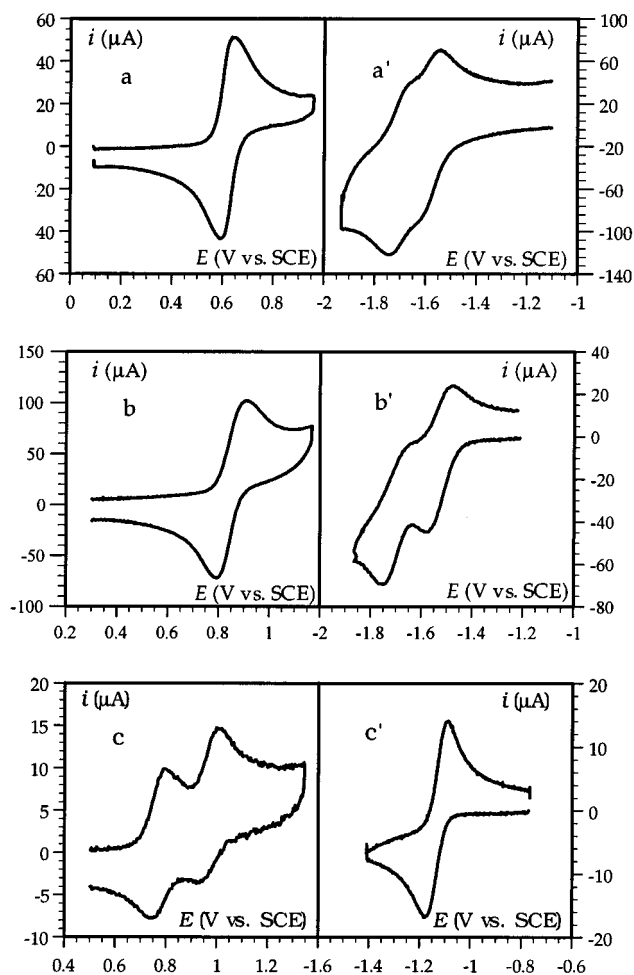


**Figure 1.** Oxidative (a, b, c) and reductive (a', b', c') voltammetry on a 1-mm-diameter disk Au electrode of **1** (a, a', 1 mM), **3** (b, b', 0.9 mM), and **2** (c, c', 0.4 mM) in  $\text{CH}_2\text{Cl}_2 + 0.1 \text{ M NBu}_4\text{PF}_6$ . Scan rate: 10 (a, c, c'), 50 (b, b'), and 200 V/s (a').

The removal of the second electron is accompanied by important structural changes, often involving the release of steric constraints.<sup>12,13</sup>

The purpose of the work reported below was first the quantitative determination of the standard potentials of uptake or removal of the first and second electrons by or from the three carotenoid molecules shown in Chart 1 including the cases where a single two-electron wave is observed. Our second objective was more general, namely, the understanding of the factors that govern the possibility that the uptake or removal of the second electron may be thermodynamically easier than the first in polyconjugated systems in which, as in carotenoids, steric constraints are absent or minor. Such systems are likely candidates for use as molecular wires. With the help of quantum chemical calculations, the discussion will mostly concern

(12) (a) For a recent comprehensive review, see: Reference 12b. See also: Reference 12c. (b) Evans, D. H.; Lehmann, M. W. *Acta Chem. Scand.* **1999**, *53*, 765. (c) Evans, D. H.; O'Connell, K. M. In *Conformational Change and Isomerization Associated with Electrode Reactions in Electroanalytical Chemistry*; Bard, A. J., Ed.; Marcel Dekker: New York, 1986; Vol. 14, pp 113–207.

(13) (a) Evans, D. H.; Hu, K. *J. Chem. Soc., Faraday Trans.*, **1996**, *92*, 3983. (b) Hu, K.; Evans, D. H. *J. Phys. Chem.* **1996**, *100*, 3030. (c) Hu, K.; Evans, D. H. *J. Electroanal. Chem.* **1997**, *423*, 29. (d) Dümming, S.; Speiser, B.; Kuhn, N.; Weyers *Acta Chem. Scand.* **1999**, *53*, 876. (e) Hong, S. H.; Evans, D. H.; Nelsen, S. F.; Ismagilov, R. F. *J. Electroanal. Chem.* **2000**, *486*, 75. (f) Bellec, N.; Boubekeur, K.; Carlier, R.; Hapiot, P.; Lorcay, D.; Tallec, A. *J. Phys. Chem. A* **2000**, *104*, 9750

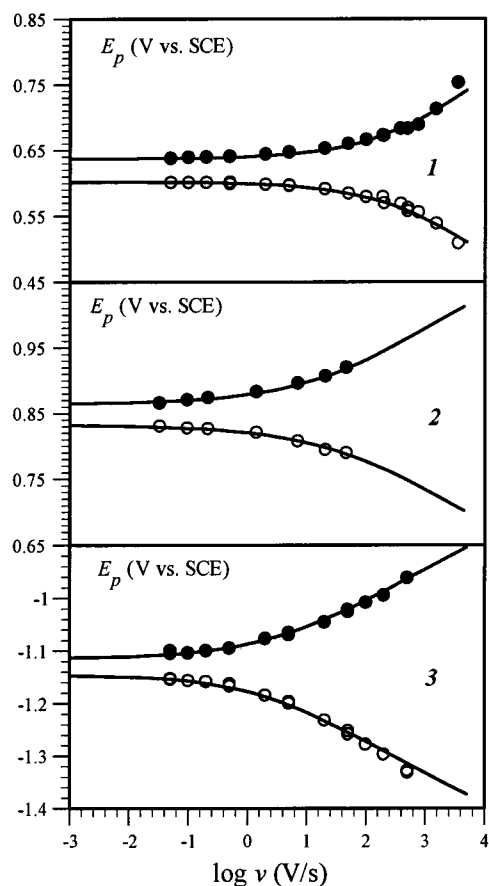


**Figure 2.** Anodic (●) and cathodic (○) peak potentials for the two-electron oxidation of **1** (0.9 mM) and of **2** (0.9 mM) and the reduction of **3** (0.8 mM) in  $\text{CH}_2\text{Cl}_2 + 0.1 \text{ M NBu}_4\text{PF}_6$  as a function of scan rate. The solid lines represent the best fit with theory as detailed in the text. Temperature, 20 °C.

**Table 1.** Thermodynamic and Kinetic Characteristics of the Two-Electron-Transfer Steps

	carotenoid		
	1	2	3
$E_{1,\text{ox}}^0$	0.634	0.875	0.775
$k_{S,1,\text{ox}}$	0.24	0.12	1.25
$E_{2,\text{ox}}^0$	0.605	0.822	0.972
$k_{S,2,\text{ox}}$	0.24	0.12	0.25
$K_{d,\text{ox}}$	3.1	7.9	$4.5 \times 10^{-4}$
$E_{1,\text{red}}^0$	-1.620	-1.634	-1.160
$k_{S,1,\text{red}}$	0.15	0.12	0.03
$E_{2,\text{red}}^0$	-1.705	-1.802	-1.100
$k_{S,2,\text{red}}$	0.15	0.1	0.03
$K_{d,\text{red}}$	$3.7 \times 10^{-2}$	$1.4 \times 10^{-3}$	10.3

$\beta$ -carotene (**1**) and canthaxanthin (**3**), but results obtained previously with other symmetrical polyenic systems will also be examined within the same conceptual framework. To uncover the effects brought about by lengthening the polyenic chain, calculations were carried out for the model systems shown in Chart 1, mimicking  $\beta$ -carotene and canthaxanthin. In this connection, our strategy was to analyze the trends appearing when the chain length is increased to uncover, in a qualitative sense, the main factors that govern the standard potential separation between the two electron-transfer reactions and thus the reasons for the appearance of an inversion between the standard potentials. The size of the systems that we are dealing with precludes a more quantitative approach.

**Table 2.** Values of  $-(RT/F) \ln K_d$  (V) Estimated from B3LYP Gas-Phase Electronic Energies and PCM Solvation Free Energies

compound	gas phase		$\text{CH}_2\text{Cl}_2$	
	ox	red	ox	red
<b>1</b>	2.35	2.42	-	-
	4.79	4.44	2.04	1.65
	3.91	3.80	1.55	1.47
	3.17	3.28	1.11	1.28
	2.88	-	-	-
<b>3</b>	2.45	2.04	-	-
	-	6.02	-	2.30
	4.61	4.44	2.08	1.50
	4.11	3.59	1.69	1.25
	3.47	3.03	1.48	0.97
	3.02	2.64	1.25	0.84

## Results

Typical cyclic voltammograms for the oxidation and reduction of **1–3** are shown in Figure 1. Beside the fact that **2** is slightly more difficult to reduce and to oxidize than **1**, the two compounds behave quite similarly in the sense that their reduction shows two separated waves whereas their oxidation shows a single two-electron wave. In contrast, **3** exhibits the opposite behavior: two successive oxidation waves and a single two-electron reduction wave.

Determination of the standard potentials is straightforward in the case of two separated waves: they are the midpoint between the anodic and cathodic peaks of each one-electron wave.

In the case of a single two-electron wave, the two standard potentials may be derived from the location of the midpoint between the anodic and cathodic peaks and the distance between them when the kinetics of the electron-transfer processes do not affect the cyclic voltammetric response. As seen in Figure 2, the distance between the two peaks increases with the scan rate, thus reflecting the increasing interference of the electron-transfer kinetics. As the scan rate decreases, the distance between the two peaks tends toward a limit, which can be regarded as a reflection of the thermodynamics of the electron-transfer process. Looking for the most accurate determination of the difference between the standard potentials, simulation of the whole voltammograms is to be preferred to the use of a working curve relating this quantity to the difference between the peak potentials extrapolated at low scan rates. Best fit simulations (DigiSim 2.1) then led to the results summarized in Table 1 (the transfer coefficients were taken as equal to 0.5 in all cases and the diffusion coefficients to  $5.5 \times 10^{-6}$ ,  $5.5 \times 10^{-6}$  and  $7 \times 10^{-6} \text{ cm}^2 \text{ s}^{-1}$  for **1**, **2**, and **3**, respectively). Estimates of the

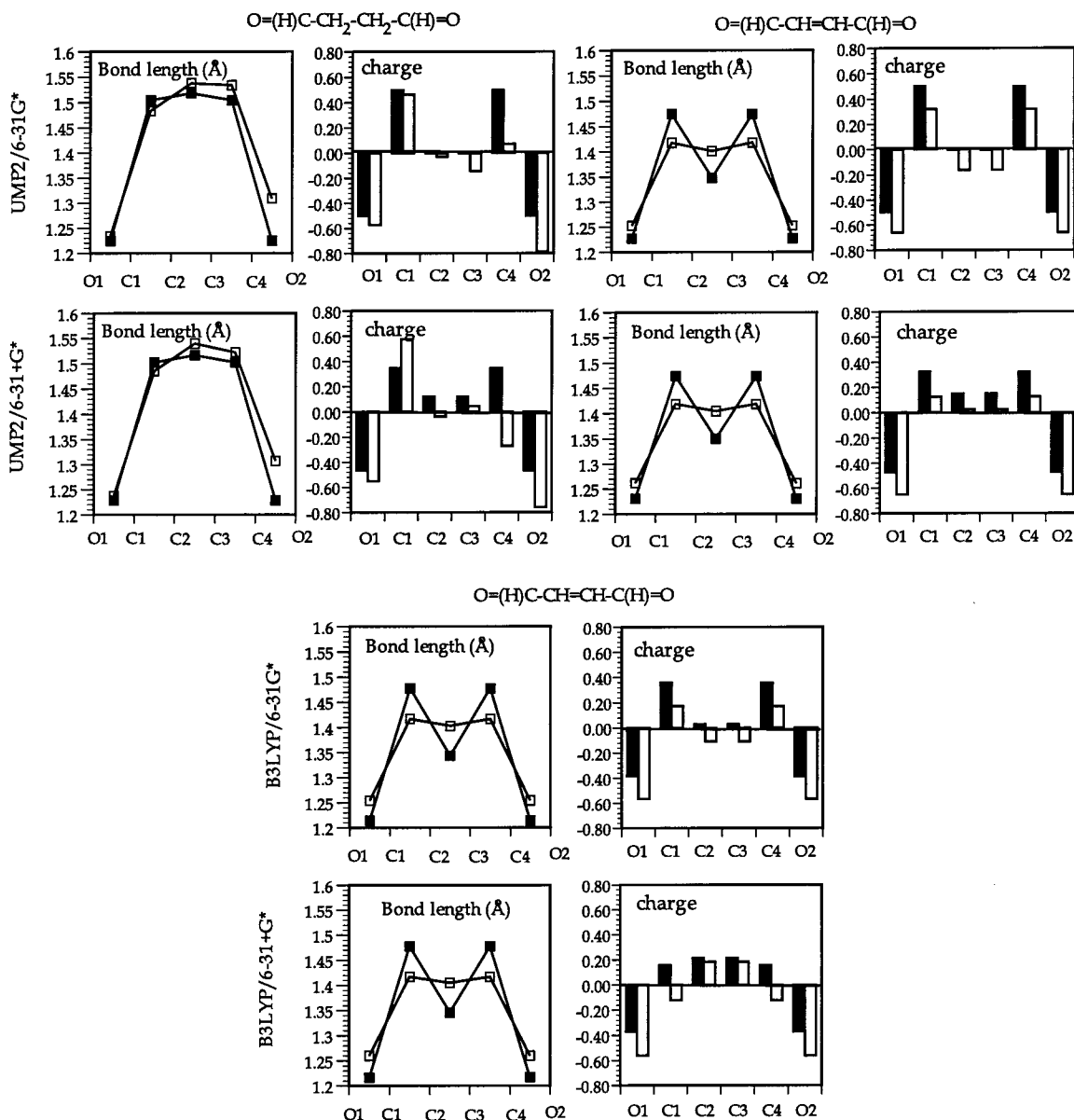


**Figure 3.** Calculated bond lengths and charges in the anion radicals (□) as compared to the neutral compounds (■) in the saturated and ethylenic four-carbon dialdehyde. Comparison of the UMP2 and B3LYP results and effect of the basis set in the case of the ethylenic four-carbon dialdehyde.

uncertainty on the difference between standard potentials for the inverted systems may be derived from the working curve relating this quantity to the difference between the peak potentials extrapolated at low scan rates.<sup>12</sup> The amount of potential inversion is thus found to be between 24 and 36 mV for the oxidation of **1**, 43 and 68 mV for the oxidation of **2**, and 47 and 80 mV for the reduction of **3**.

## Discussion

The most important aspect of the preceding results is the existence of an inversion of the standard potentials in the case of the oxidation of  $\beta$ -carotene (and also of **3**) and of the reduction of canthaxanthin, clearly beyond what is expected for two independent and distant electrophores. The structural and solvation factors explaining this behavior constitute the main objective of the following discussion. A second revealing observation is that, in the case of  $\beta$ -carotene (and of **2**), the potential inversion is observed for the oxidation while two successive steps are observed on the reduction side and that canthaxanthin exhibits the opposite behavior, namely, potential

inversion in reduction and two well-separated steps on the oxidation side.

We carried out a series of density functional (B3LYP) calculations in order to estimate the magnitude of the disproportionation equilibrium constant (eq 1) for the model compounds in Chart 1 as well as for **1** and **3**. The gas-phase results based on electronic energies are listed in Table 2.<sup>14a</sup>

The B3LYP results indicate that all radical ions have a symmetrical structure, implying that the unpaired electron and the charge are delocalized over the whole molecular framework rather than confined to one terminal group. There is a suspicion that this result might be an artifact of the method owing to the results of similar calculations carried out on the ion radicals of the saturated counterparts of the investigated polyenic molecules. In these cases, optimization either failed to go to completion or led to a symmetrical structure instead of the expected localization of the unpaired electron and charge on one of the terminal

(14) (a) The most stable structures correspond to all-trans isomers in all cases. (b) Spin contamination was only 0.764 with this short-chain polyenic compound (for additional data on spin contamination see the Experimental Section).



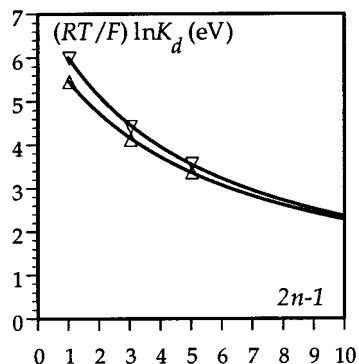


**Figure 4.** Disproportionation constant for the three first models of canthaxanthin: ▽, B3LYP/6-31G\*; △, B3LYP/6-31+G\*.

groups. To clear up the question, we carried out ab initio calculations (UHF-MP2) on one representative member of the series, namely, the anion radical of  $\text{O}=\text{(H)C}-\text{CH}=\text{CH}-\text{C}(\text{H})=\text{O}$ , for which localization in one of the terminal groups would have the best chance to occur as compared to the other members of the series.<sup>14b</sup> We also compared the results thus obtained to similar calculations of the structure of the anion radical of the corresponding saturated compound,  $\text{O}=\text{(H)C}-\text{CH}_2-\text{CH}_2-\text{C}(\text{H})=\text{O}$ , to check that the unpaired electron and charge are, as expected, located on one of the carbonyl groups. The effect of introducing diffuse functions in the basis set was also investigated. From the UMP2 results summarized in Figure 3, we may conclude that the structure of the anion radical of the conjugated molecule is indeed symmetrical with the unpaired electron and charge being delocalized over the whole molecular framework, whereas in the saturated anion radical the unpaired electron and charge are located on one of the two terminal carbonyl species. We also see that injection of diffuse functions into the basis set does not modify the above conclusion.

The introduction of diffuse functions in the basis set modifies the electronic energies as illustrated in Figure 4 by the results of B3LYP/6-31G\* and B3LYP/6-31+G\* calculations carried out on the reduction of the three first models of canthaxanthin (instability problems with the extended basis set hampered the examination of higher members of the series). It is seen that the difference between the magnitudes of the disproportionation constant obtained with and without the introduction of diffuse functions tends to vanish upon augmenting the length of the chain. The use of the B3LYP/6-31G\* methodology is thus justified, in terms of trends, for the other members of the series.

Turning back to the results for the whole set of compounds, we may note that the disproportionation constant decreases as the number of conjugated double bonds increases, meaning that the second electron-transfer step becomes easier and easier as compared to the first (Figure 5a, b). A first reason for this is the increased possibility of the two charges in the di-ion to move apart one from the other, thus resulting in a decrease of the Coulombic repulsion energy.

Another possible contribution is the structural changes taking place upon injection of a first and of a second electron, which might result in an increasing energy gain upon increasing the number of double bond. We indeed expect that passing from the neutral to the di-ion the single bonds become double bonds and vice versa. That this is indeed the case is shown in Figure 6 with the examples of  $\beta$ -carotene and canthaxanthin (In the ion radicals, the bond length is midway between the single- and double-bond values<sup>15</sup>).

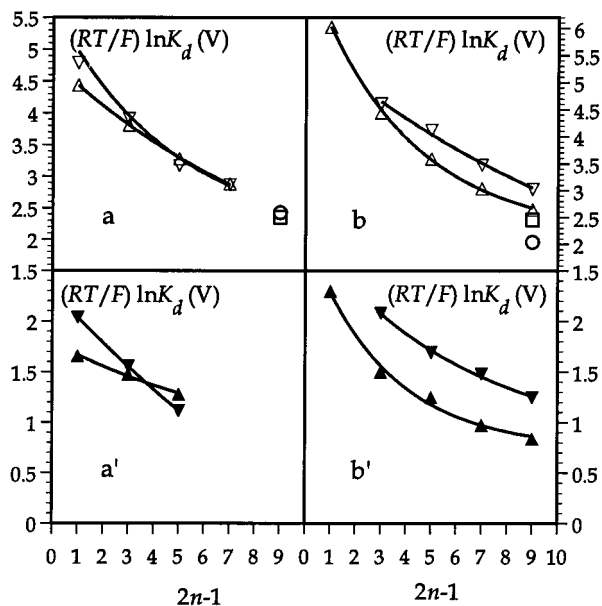


**Figure 5.** Variation of the disproportionation constant with the number of double bonds from gas-phase B3LYP (a, b) and PCM solvation (a', b') estimates: a, a' carotene (ox, □; red, ○) and model polyenes (ox, ▽, ▼; red, △, ▲). b, b' canthaxanthin (ox, □; red, ○) and model dialdehydes (ox, ▽, ▼; red, △, ▲).

This change of the molecular structure also manifests itself by the fact that the ending groups of carotene and canthaxanthin, which are not planar in the neutral compounds because of steric hindrance, tend toward planarity upon removal and addition of two electrons, respectively (Table 3).

An estimate of the effect of these structural changes on the disproportionation constants was obtained as follows. We calculated the electronic energy of the ion radical and of the di-ion when they are forced to adopt the geometry of the neutral species and compared the value of  $(RT/F) \ln K_d$  obtained under these conditions to the value derived from the optimized geometries. We also forced the neutral species and the ion radical to adopt the geometry of the di-ion and compared the value of  $(RT/F) \ln K_d$  thus obtained to the value derived from the optimized geometries. The differences thus estimated are about the same (Figure 7) and represent the effect of the structural changes on the disproportionation constants. This effect plays in favor of the inversion of the standard potentials. However, its magnitude is about the same for oxidation and reduction within each series at variance with the experimental data. For comparison,  $\Delta(RT/F) \ln K_d$  values were also calculated for two extreme situations: (i) for the reduction of 1,4-dinitroarene where large conformational changes are associated with electron transfers;<sup>13b,d</sup> (ii) for the reduction of anthracene where little conformational changes occur during reduction.<sup>13b,d</sup> With the polyenic compounds under discussion, the effects of conformational changes (Figure 7), although larger than with anthracene, remain quite modest,<sup>16</sup> definitely smaller than the effect of solvation as will appear in the foregoing discussion.

The effect of solvation was estimated by means of the PCM method (see the methodology section). The results are shown in Figure 5a' and b'. As expected, solvation considerably

(15) The calculations have been carried out with no symmetry constraints. The fact that symmetrical structures (in terms of bond lengths and charge distribution) are found confirms the correctness of the B3LYP approach in the absence of frequency calculations, which would be prohibitively lengthy for such large molecules.

(16) Although definitely larger than in the reduction of an aromatic molecule such as anthracene (Figure 6).

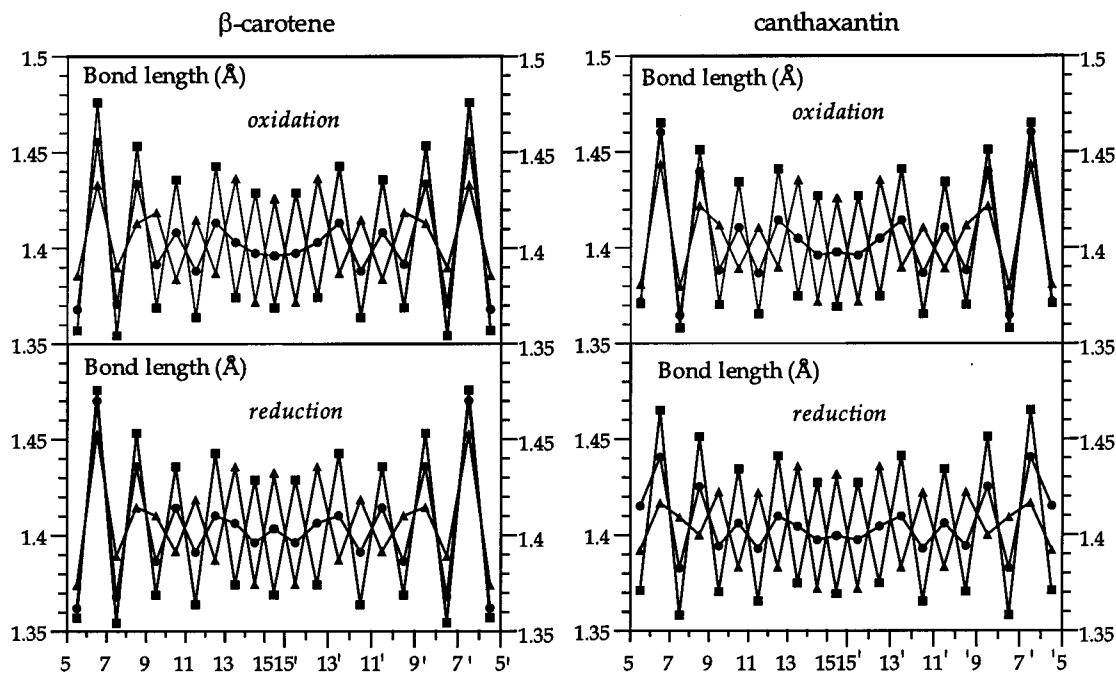


**Figure 6.** Bond lengths in  $\beta$ -carotene and canthaxanthin and their ion radicals and di-ions, from gas-phase B3LYP calculations:  $\blacksquare$ , neutral;  $\bullet$ , ion radical;  $\blacktriangle$ , di-ion.

**Table 3.** C5–C6–C7–C8 Dihedral Angle

compound	1	3
neutral	48	40
cation radical	37	39
dication	27	34
anion radical	43	23
dianion	34	7

decreases the disproportionation constant. The smallest values are obtained for the oxidation of  $\beta$ -carotene and of the longest of its model polyenes as well as for the reduction of canthaxanthin and of the longest of its model polyenic dialdehyde. They are definitely smaller than for the reduction of  $\beta$ -carotene and of its longest model polyene and the oxidation of canthaxanthin and of its longest model polyenic dialdehyde, respectively. These trends are consistent with the experimental observations. Concerning solvation effects, the charge distribution diagrams shown in Figure 8 help understand the reason for the difference in behavior of  $\beta$ -carotene (and model polyenes) and canthaxanthin (and model polyenic dialdehydes) toward oxidation and reduction.<sup>15</sup> While in the ion radicals, the charge is evenly distributed over the whole molecular framework, it tends to be concentrated in the dication of  $\beta$ -carotene and the dianion of canthaxanthin, while it remains more delocalized in the dianion of  $\beta$ -carotene and dication of canthaxanthin. The higher localization of the charges on both ends in the dication than in the dianion is also evident from the variations of the terminal bond lengths (C5–C6–C7) (see Figure 6).

Similar phenomena are observed with the two series of model compounds. They are related to the good oxidability of the terminal groups in  $\beta$ -carotene and models, due to the electron-donating properties of the methyl groups. Similarly, they are related to the good reducibility of the carbonyl groups in canthaxanthin and models. A comparison is given in Chart 2 that pictures the contribution of solvation to the difference between the standard potentials for three different situations roughly estimated by means of the Born model. For two isolated identical electrophores, there is no influence of solvation on

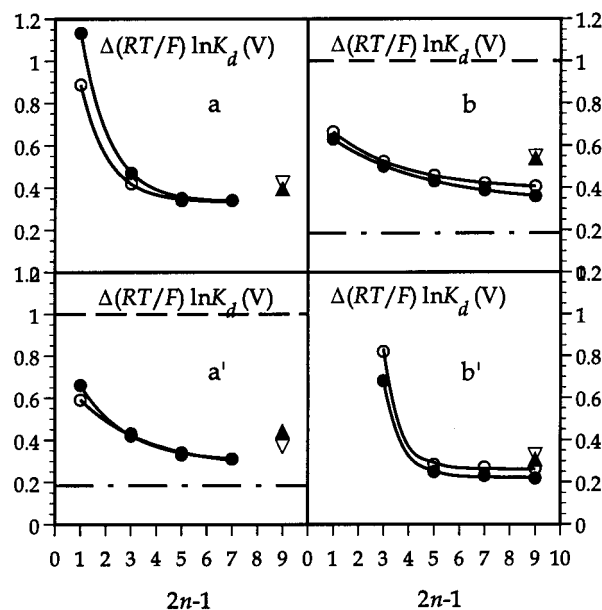


**Figure 7.** Effect of the structure changes on the disproportionation constants (see text). a, a': oxidation and reduction of  $\beta$ -carotene ( $\blacktriangle$ , geometry of the ion radical and of the di-ion as the neutral species;  $\nabla$ , geometry of the neutral species and of the ion radical and of as the di-ion) and of the model polyenes ( $\bullet$ , geometry of the ion radical and of the di-ion as the neutral species;  $\circ$ , geometry of the neutral species and of the ion radical and of as the di-ion). The horizontal lines correspond to the reduction of 1,4-dinitrodurene (---) and anthracene (- · -). b, b': reduction and oxidation of canthaxanthin ( $\blacktriangle$ , geometry of the ion radical and of the di-ion as the neutral species;  $\nabla$ , geometry of the neutral species and of the ion radical and of as the di-ion) and of the model polyenic dialdehyde ( $\bullet$ , geometry of the ion radical and of the di-ion as the neutral species;  $\circ$ , geometry of the neutral species and of the ion radical and of as the di-ion).

the standard potential difference (the contribution of solvation is the same for each). In the case of a compact molecule containing conjugated bonds, as, for example, in anthracene, solvation eases the second electron transfer, as compared to the

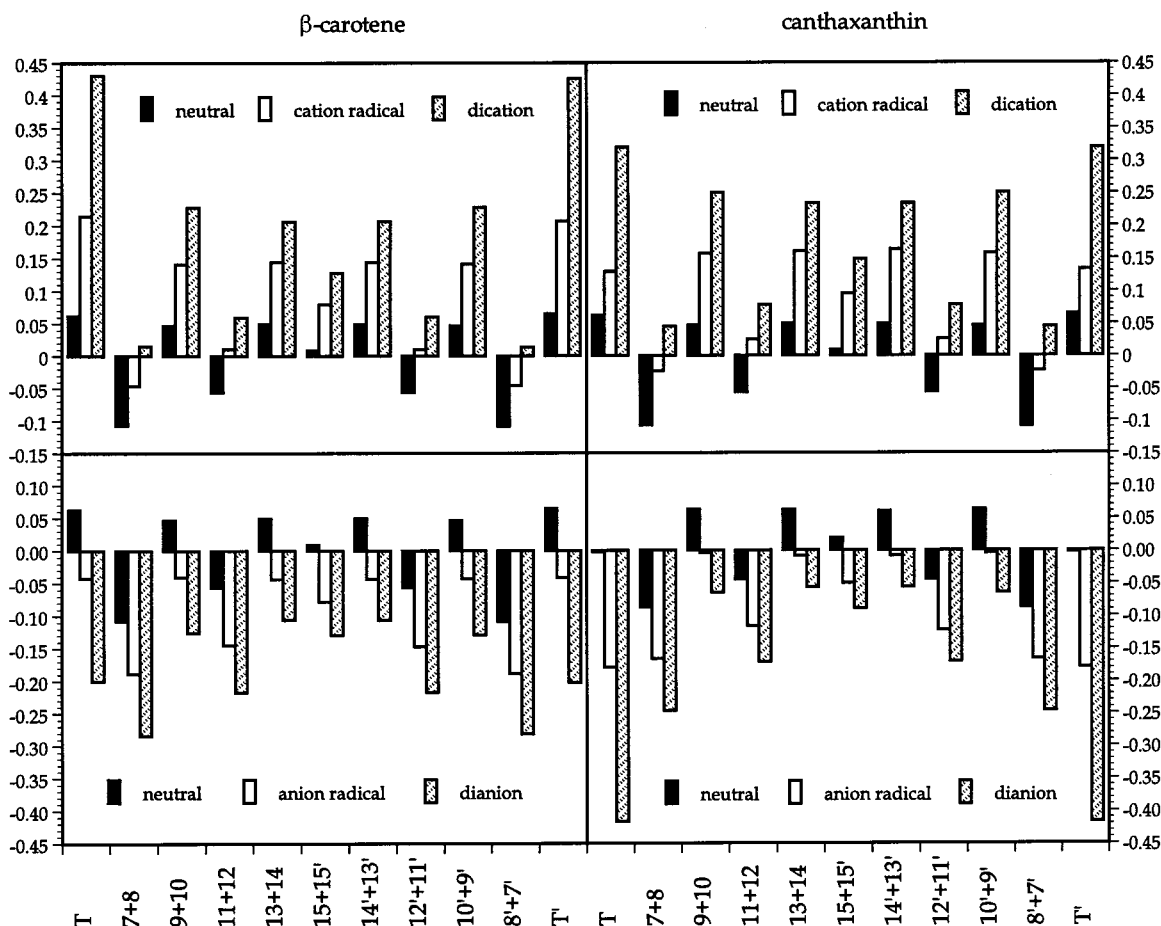


**Figure 8.** Charge distributions from B3LYP calculations. T and T' correspond to a summation involving all carbon (and oxygen) atoms beyond 7 and 7' (see Chart 1). The charges born by adjacent carbons have been summed to obtain a smoother representation of the charge distribution.

first, by the quantity  $2B/r$ , where  $r$  is the radius of the equivalent sphere and  $B$  is the Born factor (defined in Chart 2). For the present long-chain polyenic molecules, there is even more significant facilitation of the second electron transfer since, as discussed above,  $r_D < r_1$  for the oxidation of  $\beta$ -carotene and models and the reduction of canthaxanthin and models. Although the above quantum chemical analysis of the solvation effect reproduces the experimental trends correctly, it should be noted that the effect is not strong enough to lead to a potential inversion in absolute value. Besides the imperfection of the quantum chemical techniques, a likely reason for this result is that the estimate we made of solvation consisted of calculating the electrostatic energies corresponding to the charge distribution in the gas phase, structure optimization within the solvent being precluded by the large size of the investigated systems. Qualitatively, it may be envisioned that the energy gains just described are actually amplified by a synergistic effect according to the fact that the interaction with the solvent reinforces the density of charge on both ends of the di-ion.

At this stage we may conclude that the inversion of the standard potentials for the oxidation of  $\beta$ -carotene and the reduction of canthaxanthin is primarily due to the combination of two effects: (i) small Coulombic repulsion owing to the length of the molecule; (ii) concentration of the charge at both ends of the molecule (positive charge in the first case, negative charge in the second, related to the good oxidability and reducibility of the terminal groups, respectively) as compared to the ion radical, thus making solvation play against disproportionation. As compared to the case of two identical electrophores separated by a saturated chain, it is the second of these

effects that allows the inversion of the standard potentials observed with conjugated chains as opposed to saturated chains.

Before discussing the results previously obtained with other conjugated systems, we may examine the case of **2**. It behaves similarly to **1** with the difference that both the oxidations and the reductions are more difficult with **2** than with **1**. The presence of the central triple bond in **2** implies that the conjugation that may develop upon injection or removal of one and then two electrons leads to the formation of an allenic system at the center of the molecule which is less favorable energetically than the structural change taking place in **1** (Chart 3).

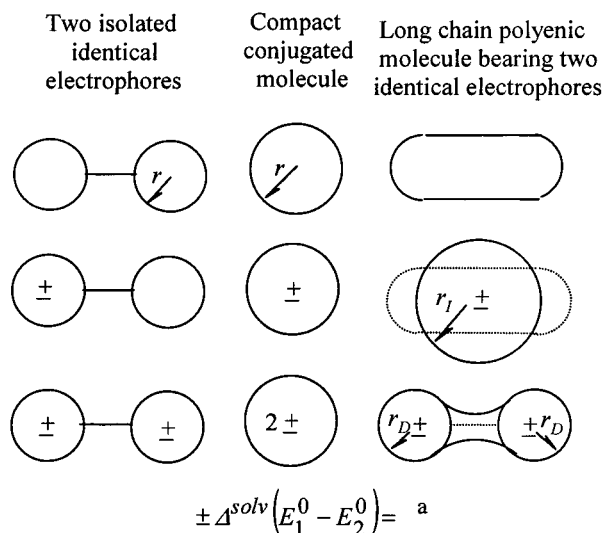
Several other organic linear and symmetrical  $\pi$ -conjugated systems have been synthesized with the aim of examining their redox behavior. Their disproportionation constants have, however, seldom been precisely determined. In the case of  $C_{26}-C_{70}$  vinylogous  $\beta$ -carotenes,<sup>8</sup> although the disproportionation constants were not measured, the voltammograms shown seem to indicate that the inversion of the standard potentials occurs when the number of double bonds is larger than in carotene itself, pointing to the applicability of the above analysis to the whole carotene family. The molecules shown at the top of Table 4 are early examples of such systems exhibiting potential

(17) Chen, C. H.; Doney, J. J.; Reynolds, G. A.; Saeva, F. D. *J. Org. Chem.* **1983**, *48*, 2757.

(18) Salbeck, J.; Schöbert, U.; Rapp, K. M.; Daub, J. Z. *Phys. Chem.* **1991**, *171*, 191.

(19) Jestin, I.; Frère, P.; Mercier, N.; Levillain, E.; Stievenard, D.; Roncali, J. *J. Am. Chem. Soc.* **1998**, *120*, 8150.

(20) Ribou, A. C.; Launay, J.-P.; Sachtleben, M. L.; Li, H.; Spangler, C. W. *Inorg. Chem.* **1996**, *35*, 3735.

Chart 2<sup>a</sup>

$$0 \quad 2B/r \quad 2B(2/r_D - 1/r_f)$$

$$B = \left( N_A e_0^2 / 4\pi\epsilon_0 \right) (1 - 1/\epsilon_S) \quad (N_A: \text{Avogadro number,}$$

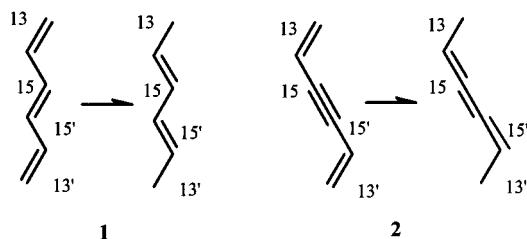
$e_0$ : electron charge,  $\epsilon_0$ : permittivity of vacuum,

$\epsilon_0$ : static dielectric constant of the solvent)

a: (+) for oxidations, (-) for reductions.

<sup>a</sup>  $B = (N_A e_0^2 / 4\pi\epsilon_0)(1 - 1/\epsilon_S)$  ( $N_A$ , Avogadro number;  $e_0$ , electron charge;  $\epsilon_0$ , permittivity of vacuum;  $\epsilon_0$ , static dielectric constant of the solvent. a, (+) for oxidations and (-) for reductions.

Chart 3



coalescence or even inversion. Other examples of organic systems where coalescence (and probably inversion) of standard potentials appears upon increasing the length of the conjugated spacers are summarized in Table 4. The case of diferrocenyl polyenes is worth an additional comment. Extrapolation of the electrochemical data gathered for  $n = 1-6$  above  $n = 6$  indicates that potential inversion should occur for larger values of  $n$ . Although the original interpretation of the data was based on Hush's model of two weakly interacting redox centers (as is often the case with mixed-valent coordination compounds), it seems likely that they are consistent with the above discussion in which charge and unpaired electron are regarded as delocalized over the whole molecular framework after removal of the first electron.<sup>21</sup> More generally, the present study emphasizes the fact that the magnitude of the disproportionation constant is not a mere reflection of the interaction between the two redox centers as often stated<sup>22</sup> despite early words of caution.<sup>23</sup>

(21) (a) Hush, N. S. *Coord. Chem. Rev.* **1985**, *64*, 135. (b) See: References 21c and d and references therein for an alternative modeling of mixed-valent complex characteristics. (c) Piepho, S. B. *J. Am. Chem. Soc.* **1988**, *110*, 6319. (d) Piepho, S. B. *J. Am. Chem. Soc.* **1990**, *112*, 4197.

(22) Fronapfel, D. S.; Woodworth, B. E.; Thorp, H. H.; Templeton, J. L. *J. Phys. Chem. A* **1998**, *102*, 5665.

Table 4. Symmetrical  $\pi$ -Conjugated Systems Showing Inversion of the Standard Potentials

System	Ref.
oxidation of:  $X = O \text{ or } S$  inversion for $n \geq 4$	17
reduction of:  R: Ph  or: 	18
oxidation of:  $n = 0, 1, 3, 5, 7$ coalescence and inversion (?) for $n \geq 3$	19
oxidation of: 	20

## Conclusions

From an experimental point of view, the most important finding is that inversion of standard potentials occurs in the oxidation of  $\beta$ -carotene and in the reduction of canthaxanthin, but not in the reduction of  $\beta$ -carotene or in the oxidation of canthaxanthin. The derivative of  $\beta$ -carotene in which the central double bond has been replaced by a triple bond shows the same characteristics as  $\beta$ -carotene in this respect. The factors that control the potential inversion in these cases as well in many other symmetrical conjugated long-chain compounds reported in the literature are essentially two. One is the weakening of the Coulombic repulsion brought about by the localization of the two charges of the di-ion at the ends of the molecules, at a

(23) (a) Sutton, J. E.; Sutton, P. M.; Taube, H. *Inorg. Chem.* **1979**, *18*, 1017. (b) Sutton, J. E.; Taube, H. *Inorg. Chem.* **1981**, *20*, 3125. (c) Richardson, D. E.; Taube, H. *Coord. Chem. Rev.* **1984**, *60*, 107.



large distance from one another. This localization is favored by a good reducibility (or oxidizability) of the terminal groups in the case of reductions or oxidations. The same factor is also, at least in part, responsible for the effect of solvation playing in favor of potential inversion. Localization of the charges in the di-ion indeed contributes to its stabilization by interaction with the solvent. In contrast, the delocalization of the charge over the whole molecular framework in the ion radical plays against its stabilization by interaction with the solvent. It is the combination of these two solvation effects that leads to potential inversion as opposed to the case where the two electrophores are linked by a saturated bridge where potential inversion cannot occur.

## Experimental Section

**Chemicals.**  $\beta$ -Carotene (**1**) was supplied by Sigma; canthaxanthin (**3**) and tetrabutylammonium hexafluorophosphate (puriss quality) were from Fluka. All carotenoids were purified by column chromatography on silica gel. Purity of the samples was checked by  $^1\text{H}$  NMR (360 MHz,  $\text{CDCl}_3$ ) and TLC analyses. The carotenoids were stored in the dark at  $-14^\circ\text{C}$  in desiccators containing activated  $\text{CaSO}_4$  and were allowed to warm to room temperature just before use.  $\text{CH}_2\text{Cl}_2$  was from Aldrich (anhydrous, 99+%). The samples were prepared in a drybox under nitrogen.

**Electrochemical Experiments.** All cyclic voltammetry experiments were carried out at  $20^\circ\text{C}$  using a cell equipped with a jacket allowing circulation of water from the thermostat. The counter electrode was a Pt wire, and the reference electrode an aqueous saturated calomel electrode with a salt bridge containing the supporting electrolyte. The SCE electrode was checked against the ferrocene/ferricinium couple (considering the following  $E^\circ = 0.528\text{ V}$  in  $\text{CH}_2\text{Cl}_2$  vs aqueous SCE) before and after each experiment. Based on repeated measurements, absolute errors of potentials were found to be around  $\pm 5\text{ mV}$ . In situations of inverted potentials,  $\Delta E_p$  measurements (which do not require the standardization of the reference electrode) were repeated at least 10 times and averaged.

The working electrode was an Au (1 mm) disk. Several tests were performed with other electrodes (Pt, glassy carbon) and similar behavior was observed. The electrode was polished before each set of voltammograms with  $1\text{-}\mu\text{m}$  diamond paste and ultrasonically rinsed in absolute ethanol. Electrochemical instrumentation consisted of a PAR model 175 Universal programmer and a home-built potentiostat equipped with a positive feedback compensation device.<sup>24</sup> The data were acquired with a 310 Nicolet oscilloscope. For high scan rate cyclic voltammetry ( $v = 100\text{--}1000\text{ V/s}$ ), a platinum ( $10\text{-}\mu\text{m}$  diameter) ultramicroelectrode was used. It was made with a wire sealed in soft glass.<sup>25</sup> The signal generator was a Hewlett-Packard 3314A, and the curves were recorded with a 4094C Nicolet oscilloscope with a minimum acquisition time of 5 ns/point.

(24) Garreau, D.; Savéant, J.-M. *J. Electroanal. Chem.* **1972**, *35*, 309.

Solutions were purged with argon before the measurements, and argon was allowed to flow under the solution during the measurements. The concentration of carotenoids was  $\sim 10^{-3}\text{ mol L}^{-1}$ ; the supporting electrolyte was tetrabutylammonium hexafluorophosphate ( $0.1\text{ mol L}^{-1}$ ).

Numerical simulations of the voltammograms were performed with the commercial BAS DigiSim Simulator 2.1<sup>26</sup> using the default numerical options with the assumption of planar diffusion. Butler–Volmer law was considered for the electron-transfer kinetics (see text). The coefficient,  $\alpha$ , was taken as 0.5 and the diffusion coefficients were assumed to be equal for the all species ( $D = 10^{-5}\text{ cm}^2\text{ s}^{-1}$ ).

## Methodology for Quantum Chemical Calculations

Geometry optimizations and energy calculations were performed with the Gaussian 98 package.<sup>27</sup> For the smaller polyenes, we checked that the geometry obtained with density functional B3LYP<sup>28</sup> with the 6-31G\*<sup>29</sup> basis set were real minimums on the energy surface by performing frequency calculations. For B3LYP calculations, spin contaminations remain negligible even for the longest polyenic compounds as shown by the low  $s^2$  values in the range 0.76–0.82; for example,  $s^2 = 0.80$  and 0.79, for **1** and **3** radical anions and 0.81 and 0.82 for the corresponding radical cations. Solvation free energies were calculated on the gas-phase optimized conformations according to the self-consistent reaction field (SCRf) method using the polarized continuum (overlapping spheres) model (PCM).<sup>30</sup>

**Acknowledgment.** We thank Hoffmann-La Roche Ltd., Basel, Switzerland, for a gift of **2**. The work at The University of Alabama was supported by the Division of Chemical Sciences, Office of Basic Energy Sciences of the U.S. Department of Energy under Grant DEFG02-86-ER13465.

JA0106063

(25) Andrieux, C. P.; Garreau, D.; Hapiot, P.; Pinson, J.; Savéant, J.-M. *J. Electroanal. Chem.* **1988**, *243*, 321.

(26) Rudolph, M.; Reddy, D. P.; Felberg, S. W. *Anal. Chem.* **1994**, *66*, 589A.

(27) Gaussian 98 (Revision A.1). Frisch, M. J.; Trucks, G. W.; Schlegel, H. B.; Scuseria, G. E.; Robb, M. A.; Cheeseman, J. R.; Zakrzewski, V. G.; Montgomery, J. A.; Stratmann, R. E.; Burant, J. C.; Dapprich, S.; Millam, J. M.; Daniels, A. D.; Kudin, K. N.; Strain, M. C.; Farkas, O.; Tomasi, J.; Barone, V.; Cossi, M.; Cammi, R.; Mennucci, B.; Pomelli, C.; Adamo, C.; Clifford, S.; Ochterski, J.; Petersson, G. A.; Ayala, P. Y.; Cui, Q.; Morokuma, K.; Malick, D. K.; Rabuck, A. D.; Raghavachari, K.; Foresman, J. B.; Cioslowski, J.; Ortiz, J. V.; Stefanov, B. B.; Liu, G.; Liashenko, A.; Piskorz, P.; Komaromi, I.; Gomperts, R.; Martin, R. L.; Fox, D. J.; Keith, T.; Al-Laham, M. A.; Peng, C. Y.; Nanayakkara, A.; Gonzalez, C.; Challacombe, M.; Gill, P. M. W.; Johnson, B. G.; Chen, W.; Wong, M. W.; Andres, J. L.; Head-Gordon, M.; Replogle, E. S.; Pople, J. A. Gaussian, Inc., Pittsburgh, PA, 1998.

(28) Becke, A. D. *J. Chem. Phys.* **1993**, *98*, 5648.

(29) Hariharan, P. C.; Pople, J. A. *Chem. Phys. Lett.* **1972**, *16*, 217.

(30) (a) Cossi, M.; Barone, V.; Cammi, R.; Tomasi, J. *Chem. Phys. Lett.* **1996**, *255*, 327. (b) For a general review about solvation methods, see: Cramer, J. Truhlar, D. G. *Chem. Rev.* **1999**, *99*, 2161.